

## Spatially resolved electron energy loss spectroscopy on n-type ultrananocrystalline diamond films

R. Arenal, O. Stephan, P. Bruno, and D. M. Gruen

Citation: *Appl. Phys. Lett.* **94**, 111905 (2009); doi: 10.1063/1.3095663

View online: <http://dx.doi.org/10.1063/1.3095663>

View Table of Contents: <http://apl.aip.org/resource/1/APPLAB/v94/i11>

Published by the [American Institute of Physics](http://www.aip.org).

---

### Related Articles

Site-specific mapping of transition metal oxygen coordination in complex oxides  
*Appl. Phys. Lett.* **101**, 241910 (2012)

Quantitative phase imaging of electron waves using selected-area diffraction  
*Appl. Phys. Lett.* **101**, 234105 (2012)

Removing the effects of elastic and thermal scattering from electron energy-loss spectroscopic data  
*Appl. Phys. Lett.* **101**, 183112 (2012)

High resolution electron energy loss spectroscopy of clean and hydrogen covered Si(001) surfaces: First principles calculations  
*J. Chem. Phys.* **137**, 094701 (2012)

Nazca Lines by La ordering in  $\text{La}_{2/3-x}\text{Li}_3\text{TiO}_3$  ion-conductive perovskite  
*Appl. Phys. Lett.* **101**, 073903 (2012)

---

### Additional information on *Appl. Phys. Lett.*

Journal Homepage: <http://apl.aip.org/>

Journal Information: [http://apl.aip.org/about/about\\_the\\_journal](http://apl.aip.org/about/about_the_journal)

Top downloads: [http://apl.aip.org/features/most\\_downloaded](http://apl.aip.org/features/most_downloaded)

Information for Authors: <http://apl.aip.org/authors>

## ADVERTISEMENT

**AIP** | Applied Physics  
Letters

**SURFACES AND INTERFACES**  
Focusing on physical, chemical, biological, structural, optical, magnetic and electrical properties of surfaces and interfaces, and more...

**ENERGY CONVERSION AND STORAGE**  
Focusing on all aspects of static and dynamic energy conversion, energy storage, photovoltaics, solar fuels, batteries, capacitors, thermoelectrics, and more...

**EXPLORE WHAT'S NEW IN APL**

**SUBMIT YOUR PAPER NOW!**

## Spatially resolved electron energy loss spectroscopy on *n*-type ultrananocrystalline diamond films

R. Arenal,<sup>1,2,a)</sup> O. Stephan,<sup>3</sup> P. Bruno,<sup>2</sup> and D. M. Gruen<sup>2</sup>

<sup>1</sup>Laboratoire d'Etude des Microstructures, CNRS-ONERA, 92322 Châtillon, France

<sup>2</sup>Materials Science Division, Argonne National Laboratory, Illinois 60439, USA

<sup>3</sup>Laboratoire de Physique des Solides, UMR CNRS 8502, Université Paris-Sud, 91405 Orsay, France

(Received 20 December 2008; accepted 14 February 2009; published online 17 March 2009)

The addition of nitrogen to the synthesis gas during synthesis of ultrananocrystalline-diamond (UNCD) films results in films uniquely exhibiting very high *n*-type electrical conductivity even at ambient temperatures. This result is due to the formation of nanowires having elongated diamond core nanostructures and a  $sp^2$ -bonded C sheath surrounding the core. The work presented here provides detailed confirmation of this important result through spatially resolved-electron energy loss spectroscopy. The direct observation of nitrogen incorporated in the sheath has been enabled. The incorporation of this nitrogen provides strong support to a plausible mechanism for the *n*-type conduction characteristic of the UNCD films. © 2009 American Institute of Physics.

[DOI: 10.1063/1.3095663]

Carbon nanomaterials such as fullerenes and nanotubes have attracted much scientific interest in the last twenty years.<sup>1</sup> More recently UNCD films have also shown outstanding properties leading to practical applications in areas such as microelectro-mechanical resonators, as well as in biology.<sup>2,3</sup> Recently, we reported for the first time the formation of diamond nanowires (NWs) in *n*-type UNCD films.<sup>4</sup> However, important aspects of their structure could not be ascertained. In particular the location as well as the atomic configuration of the incorporated nitrogen in the C network was not known. Such knowledge is crucial to the elaboration of a detailed mechanism concerning the highly unusual *n*-type conduction seen in these films.

UNCD films are synthesized from argon microwave plasmas containing 1% C in the form of  $C_{60}$  or  $CH_4$  and are highly electrically insulating.<sup>2</sup> The progressive substitution of  $N_2$  for argon in the synthesis gas renders the films increasingly electrically conducting with conductivities reaching several hundred S/cm for 20% by volume of  $N_2$  added to the synthesis gas.<sup>4-8</sup> In our recent work, we have shown that such electronic modifications, which are strongly correlated with the increase in  $N_2$  gas contents, are accompanied by morphological changes. For more than 10% by volume of  $N_2$  added to the synthesis gas we observed the formation of diamond NWs.<sup>4</sup> The aspect ratio (length/diameter) of the nano-objects is 20/30, with diameters ranging from 5 to 8 nm. In that earlier work, it was also suggested that the  $sp^2$ -bonded C sheath enveloping each NW is largely responsible for the high conductivity of these films. Here we present a detailed spatial-resolved electron energy loss spectroscopy (SR-EELS) study on these UNCD *n*-type films with special emphasis on the location and bonding of nitrogen in the  $sp^2$  carbon sheath.

As is well known, EELS is a very useful technique to investigate materials providing access to chemical composition, atom coordination, and bonding configuration with nanoscale spatial resolution.<sup>9</sup> EEL spectra were recorded using a VG-HB501 dedicated scanning transmission electron

microscope (STEM) instrument equipped with a cold field emission gun, operated at 100 keV with an energy resolution close to 0.7–0.8 eV in the core-loss region and a probe size of approximately 0.5 nm. Convergence angle on the sample and collection angle of the spectrometer were 15 and 24 mrad, respectively. This spectroscopic information was obtained using the spectrum-imaging (SPIM) acquisition mode.<sup>10,11</sup>

Plan view TEM samples were prepared following a standard procedure.<sup>4</sup>

Figure 1 shows two TEM micrographs, a low magnification image, and a high resolution TEM (HRTEM) one, respectively, recorded on one of the UNCD films synthesized with an addition of 10% of  $N_2$  to the plasma. These micrographs display the composite and complex structure of the diamond NWs embedded in a matrix formed by UNCD material.<sup>4,12</sup> The (111) lattice fringes of the diamond elongated crystallites [Fig. 1(b)] are clearly visible as well as the surrounding  $sp^2$  layer. It can be seen that the cores are composed of several 5–10 nm long segments.

Figure 2(a) displays a high-angle annular dark field (HAADF) image acquired in a hole of the TEM sample where several elongated crystallites are observed. Attention

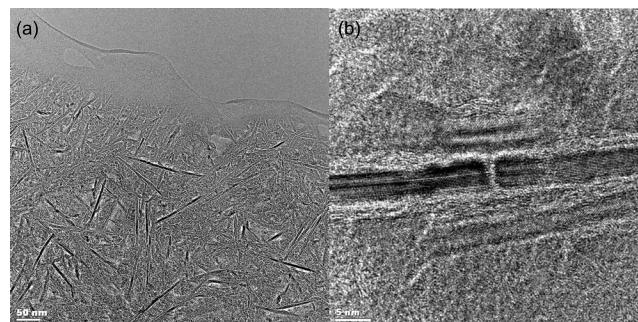


FIG. 1. (a) Low-magnification TEM micrograph recorded on an *n*-type UNCD film showing the presence of elongated crystallites (NWs, see text). (b) HRTEM image displaying a few of these NWs. The (111) diamond lattice fringes are visible, as well as the segments composing these structures.

<sup>a)</sup>Electronic mail: raul.arenal@onera.fr.

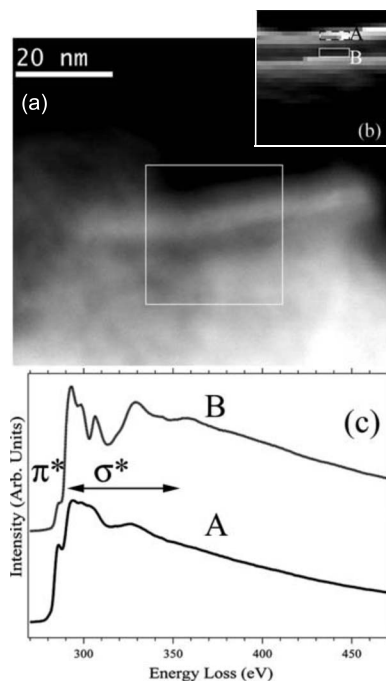


FIG. 2. (a) STEM HAADF image of an UNCD film where several diamond NWs can be observed. The white box shows the region from which an EELS SPIM was acquired. (b) EELS C  $K$   $\pi$  peak intensity map extracted from the SPIM in (a). (c) Two different EEL spectra showing the C  $K$  edge, recorded in the areas A and B as marked in (b).

is drawn particularly to one crystallite near the middle of the HAADF image. In the square area marked in the HAADF image, we recorded, along with the image, a SPIM consisting of  $32 \times 32$  individual EELS spectra. The acquisition time for each spectrum was 2 s. In C materials the analysis of the near edge fine structures (ELNES) of the C  $K$  edge allows to easily discern between  $sp^2$ - or  $sp^3$ -bonded carbons.<sup>13</sup> In fact, the  $sp^2$ -bonded carbons are clearly identified since they display a  $\pi^*$  peak at 285 eV, which corresponds to transitions of the C  $1s$  electron to the empty  $\pi^*$  antibonding orbitals, being associated with planar  $sp^2$  hybridization. Concerning  $sp^3$  bonding C, the typical features are the peak centered  $\sim 289$  eV due to the C  $1s \rightarrow \sigma^*$  transitions and the signature assigned to the second absolute gap in the diamond band structure at  $\sim 302$  eV. Thus, Fig. 2(b) shows the mapping of the  $\pi^*$  peak extracted from the recorded three-dimensional-SPIM data cube. From this figure, one deduces that  $sp^2$ -bonded C surrounds the elongated crystallite. Figure 2(c) displays the EEL spectra extracted from two different areas of the SPIM. These areas are marked in the  $\pi^*$  map, see Fig. 2(b), and correspond to the edge and to the middle of the elongated crystallite, respectively. The analysis of the fine structures of the C  $K$  edge confirms that the spectrum recorded at the edge of the NW [at the bottom of Fig. 2(c)] corresponds to  $sp^2$ -bonded C, and that the other one, extracted from the middle of the NW [at the top of Fig. 2(c)], is attributed to  $sp^3$ -bonded C with a minor contribution at 285 eV of  $sp^2$ -bonded C from the surface of the crystallite. Thus, these results strongly support the assumption that the UNCD NWs consist of a diamond core covered by a  $sp^2$ -C sheath.

In earlier work it was shown that<sup>5,12</sup> for 10%  $N_2$  in the synthesis gas the number of nitrogen atoms is about  $1.5 \times 10^{20}/\text{cm}^3$ . However, only about 1% of the  $N_2$  added to the gas phase is incorporated into the UNCD films as determined

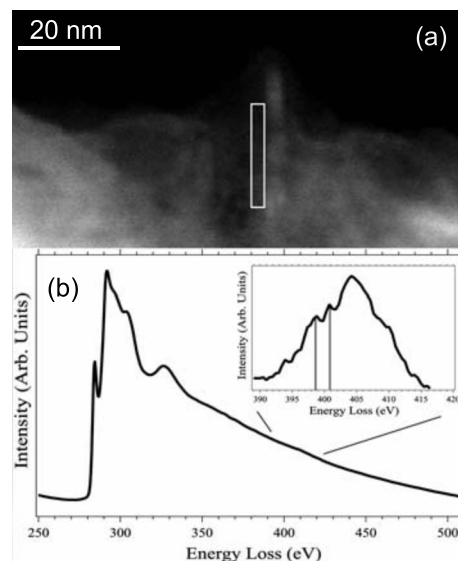


FIG. 3. (a) STEM HAADF image of a different area of the sample. (b) EELS spectra recorded in the white area marked in (a). In this spectrum, C  $K$  and N  $K$  edges are visible at  $\sim 284$  and 397 eV, respectively. The inset is a magnification of the N  $K$  edge, after background subtraction.

by secondary ion mass spectroscopy measurements. Despite strenuous efforts, until now no information is available on the precise location or bonding of the incorporated N.

In order to investigate both aspects, we performed EELS measurements using an acquisition mode consisting of rastering a slightly defocused probe over nanometer size areas at the surface of the sample and acquiring and average spectrum from the rastered area. This acquisition mode allows one to optimize the detection of very low concentrations of N atoms while reducing radiation damage effects for a detailed analysis of the N  $K$  edge ELNES. Figure 3(a) shows a HAADF image of another area where several NWs are observed. The white rectangle in this HAADF image circumscribes the area, corresponding to the edge of one of these NWs, which was analyzed by spectroscopically rastering the slightly defocused electron probe. The sum of 40 averaged spectra recorded in this area is displayed in Fig. 3(b). In this spectrum the N  $K$  edge is observed [inset Fig. 3(b)].

In order to estimate the N content we used the Hartree–Slater model to compute the ionization cross sections for the N  $K$  and C  $K$  edges.<sup>9</sup> The characteristic signals were extracted from the noncharacteristic background by the fitting method using the conventional power-law energy dependence. We found the N content to be approximately 1.5 at. %. The same procedure was used to quantify the spectra shown in Fig. 2(c). Thus, we found that the nitrogen content in the spectra recorded in the  $sp^2$  region (area A) was 0.5 at. % while it was below the detection limits of  $\leq 0.1$  at. % for the area corresponding to the  $sp^3$  C composing the core of the NW (region B). However we cannot exclude that small fraction of N could be incorporated in the tetrahedral carbon network. Furthermore, we believe that the acquisition mode employed to record the spectra shown in Fig. 2(b) is not capable quantitatively to analyze the ELNES of N  $K$  edge because the signal/noise ratio in these spectra is too low. Our SR-EELS result is the first definitive demonstration of the presence of N in the  $sp^2$ -bonded C surrounding the diamond NWs and confirms the idea proposed by Zapol *et al.*<sup>14</sup> These authors had suggested on energetic grounds

that  $N$  was not doped into the diamond crystallites but was located in the grain boundaries and interfaces among diamond crystallites. Earlier, we also had suggested that  $N$  accumulates at the grain boundaries, perhaps in the form of a copolymeric sheath,<sup>4</sup> impeding the growth of diamond grains, thus forcing the creation of secondary nucleation sites resulting in diamond NW growth.

The formation of a copolymerlike  $sp^2$ -bonded sheath could be involved in the formation both of the segments of diamond composing the NW cores [Fig. 1(a)] as well serve as an effective template for the formation of the NWs themselves. It would carry us too far afield to discuss in detail the role of  $N_2$  additions in promoting the copolymerization of pyridine and polyacetylene for example. However it seems reasonable to assume that activated nitrogen in the methane plasmas strongly favors activated  $N$  in the methane gases during the synthesis of these UNCD films strongly favors  $sp^2$ -bonded C, as recently showed by Raman spectroscopy studies.<sup>15</sup>

The inset of Fig. 3(b) shows the N  $K$  edge fine structure in detail. The  $\pi^*$  peak is split into two distinct peaks with maxima at  $\sim 398.8$  and  $\sim 401$  eV, respectively. These features were only slightly detected by Birrell *et al.*<sup>12</sup> Thus, we cannot exclude that the N can be incorporated in other configurations in these films, in particular,  $sp^3$  configuration in the tetrahedral C network, as the works of Birrell *et al.*<sup>12</sup> indicated. It should be noted that the difference between our present results and those of Birrell *et al.*<sup>12</sup> can be explained by the differences among the techniques employed to get them which are, in fact, complementary. We used SR-EELS, which is a local probing method, and Birrell *et al.*<sup>12</sup> performed near-edge x-ray absorption fine structure-soft x-ray fluorescence measurements, which are global and mainly surface techniques (the probing depth is few nanometers). In fact, the signal that they are recording mainly comes from the  $sp^3$ -bonded C material existing in the films to which N is associated. Furthermore, it is worth emphasizing that here we are dealing with very low amount of incorporated N, which is localized in specific and small areas. Thus, all these aspects justify the observed differences. On the other hand, a significant effort, both experimentally and theoretically, has been devoted in order to elucidate the N atomic configuration in  $CN_x$  films<sup>16</sup> because the incorporation of this N controls the properties of these films. Nevertheless it is worth mentioning that there have been widely diverging reports in the literature on how spectroscopic data should be interpreted. Hellgren *et al.*<sup>17</sup> performed a deep combined theoretical (using gradient correlated density functional theory) and experimental (x-ray absorption and emission spectroscopies) works on  $CN_x$ . They found that there are three different peaks in the N  $K$  edge at  $\sim 398.5$ , around 399.5, and  $\sim 401$  eV. They assign, helped by their simulations, these peaks to pyridine-like, a nitrile group and substituted nitrogen (graphitic). Thus, from these works, the ELNES analyses of our films [Fig. 3(b)] can be interpreted to show that  $N$  exists in two different states of chemical bonding: pyridinelike and graphitic. These two bonding configuration of nitrogen in a  $sp^2$  C network correspond to twofold coordinated  $N$  atoms neighboring a C vacancy for the pyridinelike case and to a replacement of a graphitic C atom by a nitrogen one for the

“substitutional” or “graphitic” case. It is worth mentioning that the work from Robertson and Davies<sup>18</sup> showed that among these different N atomic configurations, the substitutional configuration is the only one that can actively dope the  $sp^2$  network generating a donor state. These authors mention also the existence of pyrrolelike N configuration in  $sp^2$  C network. In such pyrrolic configuration,  $N$  is threefold coordinated in a fivefold ring. From works developed on N doped C nanotubes<sup>16</sup> the spectral feature of pyrrolelike configuration is peaking around 399–401 eV. Thus, we cannot exclude that N pyrrolic configuration could exist in less graphitic areas of the C sheaths.

In summary, we have performed spatially resolved EELS analysis on diamond NWs present in  $n$ -type UNCD films. These EELS measurements confirmed that the diamond NWs consist of two components: a nanodiamond core and a  $sp^2$  C sheath surrounding the core. We also demonstrated that nitrogen is situated in the  $sp^2$  C sheath. The amount of  $N$  is approximately 1.5 at. % and is situated in pyridinelike and graphitic configurations. Nevertheless pyrrolelike atomic arrangement cannot be excluded in less graphitized C sheaths. The results confirm that the addition of large amounts of  $N_2$  to the synthesis gas is crucial for the formation of the diamond NWs, as well as for the promotion of the  $sp^2$  aromatic clustering, for the enhancement of the ordering of these clusters and for increasing their size. Thus, a better understanding of the conditions leading to the unusual  $n$ -type electrically conducting UNCD films has been achieved.

This work was supported by the U. S. Department of Energy, Office of Science, under Contract No. DE-AC02-06CH11357.

<sup>1</sup>Carbon Nanotubes: Synthesis, Structure, Properties, and Applications, edited by M. S. Dresselhaus, G. Dresselhaus, and Ph. Avouris (Springer, Berlin, 2001).

<sup>2</sup>D. M. Gruen, *Annu. Rev. Mater. Sci.* **29**, 211 (1999).

<sup>3</sup>O. A. Shenderova and D. M. Gruen, *Ultrananocrystalline Diamond* (William Andrew, New York, 2006).

<sup>4</sup>R. Arenal, P. Bruno, D. J. Miller, M. Bleuel, J. Lal, and D. M. Gruen, *Phys. Rev. B* **75**, 195431 (2007).

<sup>5</sup>S. Bhattacharyya, O. Auciello, J. Birrell, J. A. Carlisle, L. A. Curtiss, A. N. Goyette, D. M. Gruen, A. R. Krauss, J. Schlueter, A. Sumant, and P. Zapol, *Appl. Phys. Lett.* **79**, 1441 (2001).

<sup>6</sup>J. Birrell, J. A. Carlisle, O. Auciello, D. M. Gruen, and J. M. Gibson, *Appl. Phys. Lett.* **81**, 2235 (2002).

<sup>7</sup>P. Achatz, O. A. Williams, P. Bruno, D. Gruen, J. A. Garrido, and M. Stutzmann, *Phys. Rev. B* **74**, 155429 (2006).

<sup>8</sup>O. A. Williams, *Semicond. Sci. Technol.* **21**, R49 (2006).

<sup>9</sup>R. F. Egerton, *Electron Energy-Loss Spectroscopy in the Electron Microscope*, 2nd ed. (Plenum, New York, 1996).

<sup>10</sup>C. Jeanguillaume and C. Colliex, *Ultramicroscopy* **28**, 252 (1989).

<sup>11</sup>R. Arenal, F. De la Pena, O. Stephan, M. Walls, M. Tence, A. Loiseau, and C. Colliex, *Ultramicroscopy* **109**, 32 (2008).

<sup>12</sup>J. Birrell, J. E. Gerbi, O. Auciello, J. M. Gibson, D. M. Gruen, and J. A. Carlisle, *J. Appl. Phys.* **93**, 5606 (2003).

<sup>13</sup>V. J. Keast, A. J. Scott, R. Brydson, D. B. Williams, and J. Bruley, *J. Microsc.* **203**, 135 (2001).

<sup>14</sup>P. Zapol, M. Sternberg, L. A. Curtiss, T. Frauenheim, and D. M. Gruen, *Phys. Rev. B* **65**, 045403 (2001).

<sup>15</sup>R. Arenal, G. Montagnac, P. Bruno, and D. M. Gruen, *Phys. Rev. B* **76**, 245316 (2007).

<sup>16</sup>C. P. Ewels and M. Glerup, *J. Nanosci. Nanotechnol.* **5**, 1345 (2005).

<sup>17</sup>N. Hellgren, J. Guo, C. Sathe, A. Agui, J. Nordgren, Y. Luo, H. Agren, and J.-E. Sundgren, *Appl. Phys. Lett.* **79**, 4348 (2001).

<sup>18</sup>J. Robertson and C. A. Davies, *Diamond Relat. Mater.* **4**, 441 (1995).